The Effect of Welding Parameters on the Room and High Temperature Tribological Behavior of the Weld Overlaid Die

S. Abdi [1], I. Ebrahimzadeh *[2]

Advanced Materials Research Center, Department of Materials Engineering, Najafabad Branch, Islamic Azad University, Najafabad, Iran

Abstract

As an important problem in forging factories, dies are destroyed because of high wear rate, plastic deformation and thermal and mechanical fatigue at high temperatures. This paper is an investigation into the use of nickel super alloy with different welding parameters. Three weld overlaid alloys of inconel625, as wear resistance hardfacing materials on H13 tool steel, with different welding parameters were deposited on H13 steel substrates using the tungsten inert gas welding process. Dilution, microstructures and microhardness of the weld overlays were obtained at room temperature. Wear tests were carried out using the pin-on-disk wear tester at room temperature and 550 °C. The wear surfaces were examined by scanning electron microscopy (SEM). The results showed a much lower wear at high temperature with the weld overlays welded under the pulse condition. In the performance tests, a better die life behavior was observed by using a die coated with Inconel625. The die life in the hot forging of production was increased by 86%, as compared to AISI H13 steel.

Keywords: Wear; hardfacing; Inconel625; AISI H13; Welding.

1. Introduction

Die life is an important factor in metal-forming processes used for the mass-production of metallic parts. In the mass production, the quality of tools has influence on the cost, properties and dimension of final products. The cost of final products would be reduced by an increase in the service life of the tools [1-3]. In addition, hot working tools must bear service condition such as (a) high operation temperature [≥500 °C], (b) large forming load, (c) high velocity impact, (d) repeated sliding of hot work piece, and (e) repeated thermal and mechanical tension [4]. Important reasons for the subversion of forging dies are wear, mechanical fatigue, plastic deformation and thermal fatigue, as shown in Fig. 1 [2, 4-7].

Lenge et al. reported that wear failure formed nearly

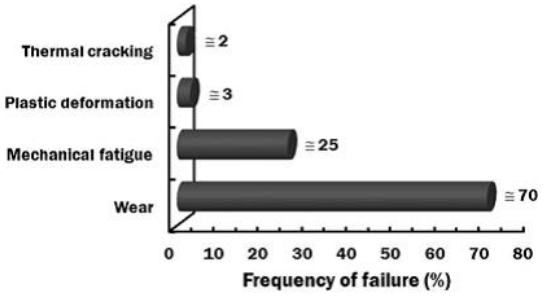

Fig. 1. Typical failures of warm and hot forming tools and its frequency [8].

* *Corresponding author*
Email: i.ebrahimzadeh@pmt.iaun.ac.ir
Address: Advanced Materials Research Center, Department of Materials Engineering, Najafabad Branch, Islamic Azad University, Najafabad, Iran
1. M.Sc.
2. Assistant Professor

70 % of the typical failure. For this reason, many researchers have been working on increasing the wear resistance of die surface [8]. Different surface techniques such as gas nitriding, plasma nitriding, CVD, PVD and duplex process improve die wear resistance [4, 9]. Ebrahimzadeh et al. studied the influence of plasma nitriding and duplex nitriding-physical vapor deposition (PVD), including two and three layer PVD coatings, on the tribological properties of AISI H13 steel at a range of temperatures. PVD coatings were deposited by a cathodic arc-PVD method on the surface of the steel pins. The performance tests demonstrated the betterment of die life, as compared to H13 hot work tool steel dies [10, 11, 12].

All these techniques can only be used for improving the life time of hot working tool steel, but the deposition of hardfacing by the welding process can also be used for the recovery of disabled tools. To reduce wear rate in hot forging dies, the dies surface hardfacing can be applied with welding, laser and direct metal rapid tooling [13].Fahrhani et al. worked on hot facing hot working tool steel (H11) using cobalt base super alloy by Tungsten Arc Welding. They reported that when the temperature was increased from room temperature to 550 °C, the wear loss was significantly reduced [5]. Kashani et al. used nickel and cobalt base super alloy as a kind of wear resistance hardfacing material on the hot working tool steel (H11) by employing Tungsten Arc Welding. They reported that Inconel625 had an acceptable wear behavior at high temperatures [14]. It is well accepted that nickel base super alloys are resistant to deformation and wear at the temperature range of

Table 1. Composition of the materials used in this research.

Material	C	Cr	Si	Mo	Fe	Ni	Other
H13	0.408	5.37	0.806	0.978	Bal.	-	1 V
Inconel625	0.03	22	-	9	1	Bal.	3.2 Nb & Ta

Table 2. Constant process parameters of cladding in this research.

Process parameter	**Constant value**
Shielding gas flow rate, 1/min	9
Filler rod diameter, mm	2.4
Electrode material	98% W + 2% Zr
Electrode diameter, mm	3.15
Mean arc voltage, V	10
Welding speed , mm/s	10
Pre heat, °C	400
Post heat, °C	550

Table 3. Welding parameters of cladding in this research.

Samples	Welding parameters
A1	Ampere=70A
A2	Ampere=100A
A3	Pulse, I_b=60A , I_p=120A frequency=60

300-500 ºC [14]. All the papers emphasize the room temperature tribology or H11 hot work tool steel, but there has been no article in the field of high temperature tribology of H13 Hot work tool steel. In addition, no study has yet investigated the influence of the welding parameters of Inconel 625 hardfacing layer on H13 die life. In this search, it has been tried to find the implementing parameters to get acceptable adherence and wear resistance at the high temperature.

2. Materials and Methods

2. 1. Materials

The substrate material used in this study was AISI H13 tool steel, which is often applied to hot forging dies. The substrate, which was cylindrical in shape (D=20 mm, H=40 mm was then prepared before cladding process so as to improve the substrate surface and remove its contaminants. The chemical composition of the H13 and Inconel625 (AWS Er NiCrMo-3) is shown in Table 1.

Three samples were deposited by Inconel 625 using tungsten inert gas welding. The H13 steel was quenched and tempered before welding. Constant and variable Parameters and conditions of welding are shown in Tables 2 and 3 respectively.

The considerable advantage of pulsed-current GTAW is the lower heat input, resulting in diminishing warpage and distortion in thin work pieces. By using the GTAW process, the weld pool and fusion zone, welding speed, weld penetration and weld quality are easily controlled, and the absorption of gases by the weld pool and hot cracking tendency can be reduced [15].

2. 2. Microstructural analysis

Microstructural examination was performed on the cross section of the deposit, in addition to the surface of the deposit. The specimens were first etched in Ferro chromic for 20 seconds.

2. 3. Dilution and heat input

The properties of the clad materials, such as mechanical strength, are impressed not only by the chemical composition of clad, but also by the clad dilution [16]. The acceptable clad dilution depends on the heat input; the heat input, in turn, depends on the welding arc voltage, current etc. In a continuous current GTAW, heat input is calculated from the continuous current, while in the pulsed process, heat input is estimated from the medium current (I_m) Fig. 2.

The heat input per unit length has a direct proportion with voltage and current; also, it is reversely proportional to the welding speed. Heat input is discussed a very important factor as it affects the dilution, bead geometry and wear properties of the clad. The medium current and

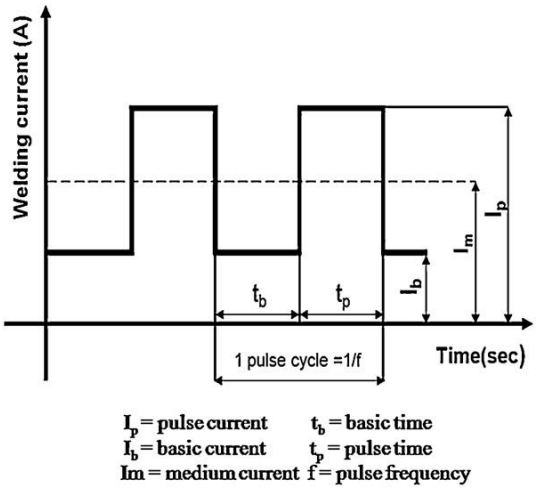

Fig. 2. Pulse GTAW process parameter [17].

heat input (HI) 18) can be calculated by Eqs. (1) and (2).

$$I_m = \frac{(I_P \times t_P) + (I_b \times t_b)}{t_P + t_b} \quad \text{Eq. (1)}$$

$$HI(Kj/mm) = \frac{I_m \times v}{s} \times \eta \quad \text{Eq. (2)}$$

, where V is voltage, S is the welding speed, and η is the efficiency of the GTAW process (usually assumed to be 60–70%) [18]. Dilution was evaluated as the area ratio of the substrate melted area and total melted area; the percentage of dilution was individually calculated using the Eq. (3) [19], as shown in Fig. 3.

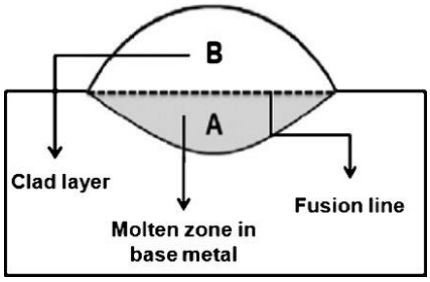

Fig. 3. Area for computing dilution.

$$D = \frac{A}{A+B} \times 100 \quad \text{Eq. (3)}$$

2. 4. Microhardness

Microhardness test was performed using Vickers indenter with a load of 300 g and dwell time of 15 s to

section the specimens radially. This condition was used on the transverse section of each weld overlay coating. Seven microhardness obtained from the fusion line to the surface at room temperature.

2. 5. Wear test

Wear tests were carried out using a pin on disk test (Fig. 4). The stationary pin specimen, 40 mm in height and 5 mm in diameter was made from AISI H13 hot work tool steel, as either not clad or hard faced with nickel super alloys. The disks were made from MO40 tool steel. The MO40 steel was selected because this counter face used for forging materials in the industry. This material was in annealing condition. The surface of the pins and the disks were prepared for the wear test. The sliding speed of 0.4 m/s, the load of 55 N (selected after load ability test), and the total sliding distance of 1000 meters were applied. The selection of these parameters was according to the real condition of forging [2)]. Wear tests were performed at two temperatures: room temperature and 550 °C. Before and after each experiment, pins and disks were weighed after cleaning. Then the weight loss by wear was measured.

Fig. 4. Pin used in pin on the disk test Manufactured from the welded zone.

2. 6. Performance test

The hot forging tests were carried out under the real working condition of a steel block (Fig. 5) in order to compare the performance of the coated and uncoated dies. The dies were machined in AISI H13 steel and coated with Inconel625, which had the best condition of welding for improving wear resistance. The die life of the dies was estimated under the same production conditions.

Fig. 5. Typical product produced with the hot forging process.

3. Results and Discussion

3. 1. Microstructure

The optical micrograph of the clad bead is presented in Fig. 6. In all cases, the microstructure of clad bead appeared to comprise mainly of columnar dendrites. However, changes in the dendrite spacing and grain structure were observed as the processing parameters varied. From the interface of clad-substrate, there was an evolution of columnar dendrites growing perpendicularly to the substrate. There was a transition to near horizontal columnar dendrites near the top region (equal to the substrate). At the clad-substrate interface, heat transfer was basically through conduction from the melt pool to the substrate.

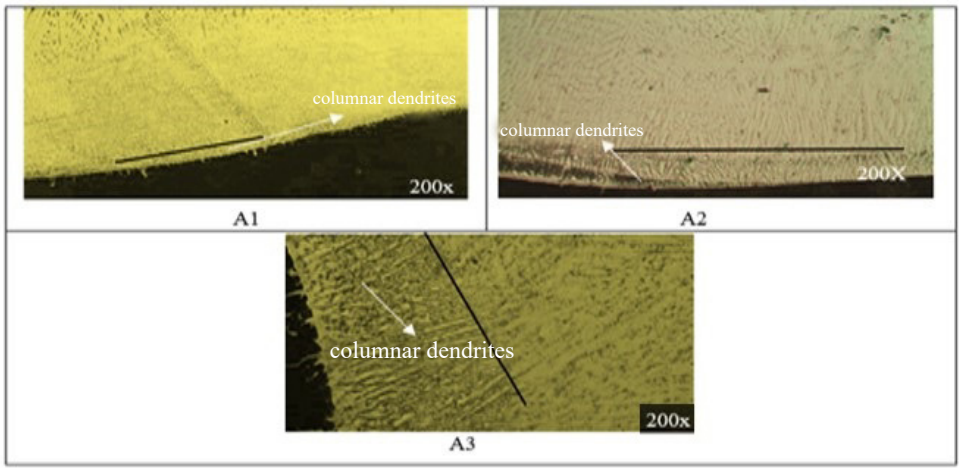

Fig 6. Microstructures of the weld overlay in (a) A1, (b) A2, (c) A3 samples.

The reason for the vertical growth of the dendrite from the substrate was because of the fact that the substrate could act as the heat sink in this region, as dendrites in FCC nickel alloys grew the fastest along the <100> directions, which was most closely aligned to the maximum temperature gradient. The growth of horizontal columnar dendrites near the surface area could be attributed to the change in the principal heat flux direction. Similar findings have been reported by Dinda et al. during the investigation of the microstructure of Inconel 625 powder laser clad [7].

3. 2. Dilution and heat in put

After welding samples were cross-section, they were prepared for taking photos with stereo microscope. Pictures of each sample shown in Fig. 7. Heat input and Dilution ratio were computed by Eqs. (2) and (3) respectively, as shown in Table 4.

According to the Fig. 7 and Table 4, it could be understood that A2 had more dilution than A1 and A3. High dilution was because of the high heat input. By increasing the ampere in welding, the mass of base metal melting could be increased, causing resonance of the dilution.

Table 4 shows that by increasing the welding ampere, the heat input to the welding piece was increased. The increment of heat input causes more melting of base metal, that resulting in an increase in dilution. By increasing the amount of dilution, the concentration of the base metal in the molten case or less than that could be achieved because of the reduced hardness.

In the case of pulse welding, although the ampere is higher compared to the A2 sample, it has less dilution. Because it did was not melt during welding, and only parts were melted in high ampere, and the low ampere was spent on cooling. This reduced dilution and increasing the hardness.

3. 3. Microhardness

The microhardness of H13 test block after quenching and tempering was 510HV. Hardness profile in the weld overlay of the hard faced test block (before the wear test)

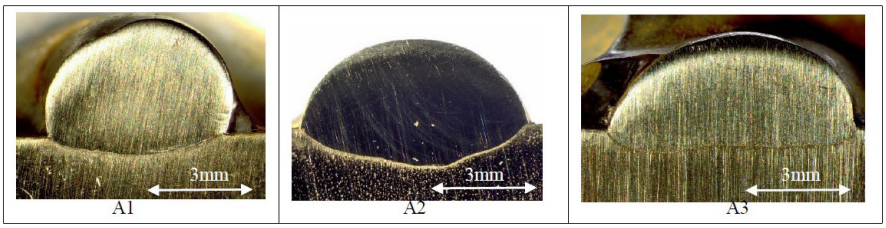

Fig. 7. Cross section image of some specimens.

Table 4. Dilution ratio, HI and hardness of each sample.

Samples	Dilution ratio (%)	HI(kJ/mm)	Microhardness
A1	13.313	42	200.13
A2	30.033	60	171.06
A3	14.007	54	190.96

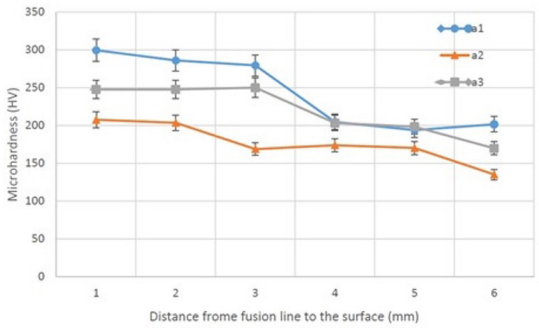

Fig. 8. Microhardness of samples at room temperature.

is shown in Fig. 8.
Fig. 8 shows the results of microhardness from the fusion line to the surface at room temperature. Sample A1 had high microhardness, followed by A3, in which there was welding with pulse condition at room temperature. The microstructure of cladded samples (Fig. 6) shows that the fine microstructure was for sample A1 that has higher hardness.

3. 4. Wear results at ambient and high temperature

Fig. 9 shows the change in weight loss for A1, A2 and A3 weld overlays and H13 hot work tool steel at both room temperature (i.e., 25 ºC) and 550 ºC, under a normal load of 55 N, the sliding speed of 0.4m/s, and the sliding distance of 1000 m. The H13 specimen showed the lowest wear with a hardness of about 480HV. Contrary to the room temperature wear, the amount of the wear of the specimens, except the uncoated H13, was decreased significantly at the higher wear temperature. Furthermore, all Inconel 625 weld overlays, which showed the highest wear at room temperature, exhibited the lowest wear at the temperature of 550 ºC. The results is consistence with the research of Farahani et al. that worked on hot facing hot working tool steel (H11) using cobalt base super alloy, by Tungsten Arc Welding, that an increase in temperature caused an improvement in wear resistance of cladded layer [5].

3. 5. The Effect of Temperature on the Friction Coefficient

Fig. 10 shows the friction traces of the Inconel 625 coated and H13 pins sliding on the Mo40 disk at room temperature. H13 without overlay had a low friction coefficient in which there were fluctuations in it. The fluc-

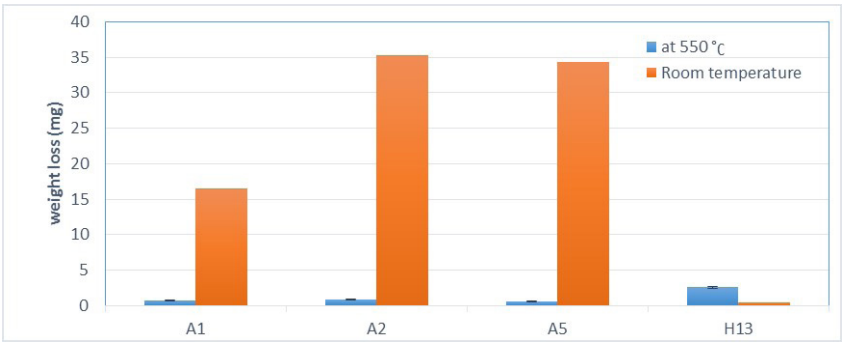

Fig. 9. Weight loss of the pin at room temperature and 550 ºC.

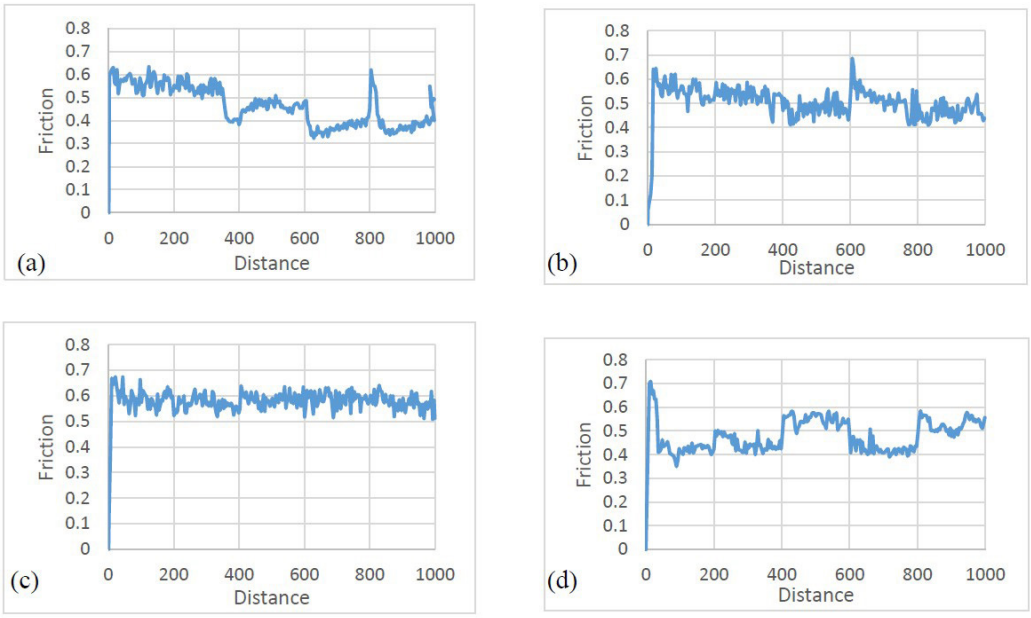

Fig. 10. Plot of friction coefficient vs. sliding distance for Inconel625 coating and H13 sliding against Mo40 disk at room temperature, (a) A1, (b) A2, (c) A3 and (d) H13 without coating.

tuations were for three samples overlaid by inconel625. Samples A1 and A2 which did not use pulse condition, had fluctuations in the friction coefficient (Fig. 10-a and Fig. 10-b), but in sample A3, where welding was under pulse condition, friction coefficient was stable (Fig. 10-c). The three- component wear was the main reason of the fluctuations in the friction coefficient at ambient temperature [10, 11].

Fig. 11 shows the friction traces of the Inconel 625 coated and H13 pins sliding on the Mo40 disk at 550 ºC. H13 without overlay had a friction coefficient of about 0.4 during the wear test. Samples overlaid with inconel625, such as A1 and A2, which did not use pulse condition, had a friction coefficient near 0.5 during the test (Fig. 11-a and Fig. 11-b), but in A3, where welding was under pulse condition, the friction coefficient was 0.4, but it increased to 0.5 at the end of the test (Fig. 11-c). Increasing the friction coefficient in A3 led to the creation of enameled and broken layers.

SEM micrographs of the wear surfaces of the welding overlays tested at 550 ºC are shown in Fig. 12. During sliding at elevated temperatures which also had a higher rate of oxides, compacted oxide layers (known as a 'glaze' [20,21]) were formed on the wear surfaces. The accumulated wear debris particles could be subsequently and compacted sintered to form solid compact layers, the tops of which were more burnished to develop smooth wear-protective layers on the wear surfaces [20]. Fig. 12c shows the SEM micrograph of the wear surface of A3, showing the lowest wear at 550 ºC (Fig. 9). Comparing A1 and A3 overlays (Figs. 12a and 12b) showed that the oxides in the compact layers became more solidly sintered together. The solid compacted layers on the weld overlays would act as smooth load-bearing areas lowering contact stresses on the wearing surfaces [20, 22, 23]. The solid compacted layers are believed to be partially responsible for the transition from the higher wear at low temperature to the lower wear at the high temperature, as observed from the results of wear test samples at room and high temperatures (Fig. 8 and 9). Fig. 12-d shows the SEM micrograph of H13 without the overlaid layer after the wear test. It seemed that there was avulsion in the surface of the pin.

In order to determine the surface layer in the wear zone of the H13 steel sample without coating and sample (with less weight loss) EDS analysis was used (Fig. 13). The analyzed zones indicated in Fig. 12-c and –d. The EDS results showed that for cladded sample less oxidation accrued, but in H13 steel iron oxide composed.

3. 7. Performance test

For the performance test, the worn die used for making the product, was overlaid with the best welding parameters. Pulse condition had the least wear at high temperatures. Fig. 14-a shows an old template having a lot of deep and continuous cracks and excessive wear on the edges. These defects were created because of the high velocity impact at high temperatures. Fig. 14-b shows the die overlaid with Inconel 625 super alloy under the pulse condition. Fig. 14-c shows the die after the performance test. According to the image, cracks in the die were greatly reduced but there were significant edge wear. H13 dies without coating and with coating produced about 3200 and 5,900 products respectively. The average service life of die was improved significantly with an increase of 86%, as compared to the H13 tool steel die.

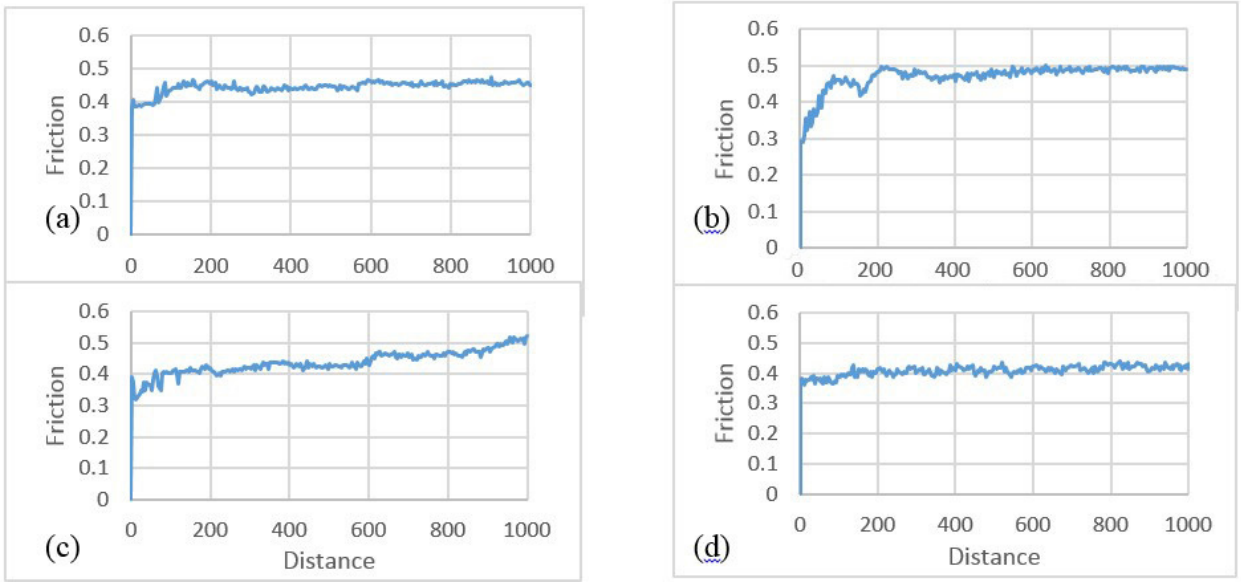

Fig. 11 Plot of friction coefficient vs. sliding distance for Inconel625 coating and H13 sliding against Mo40 disk at 550 ºC, (a) A1, (b) A2, (c) A3 and (d) H13 without coating.

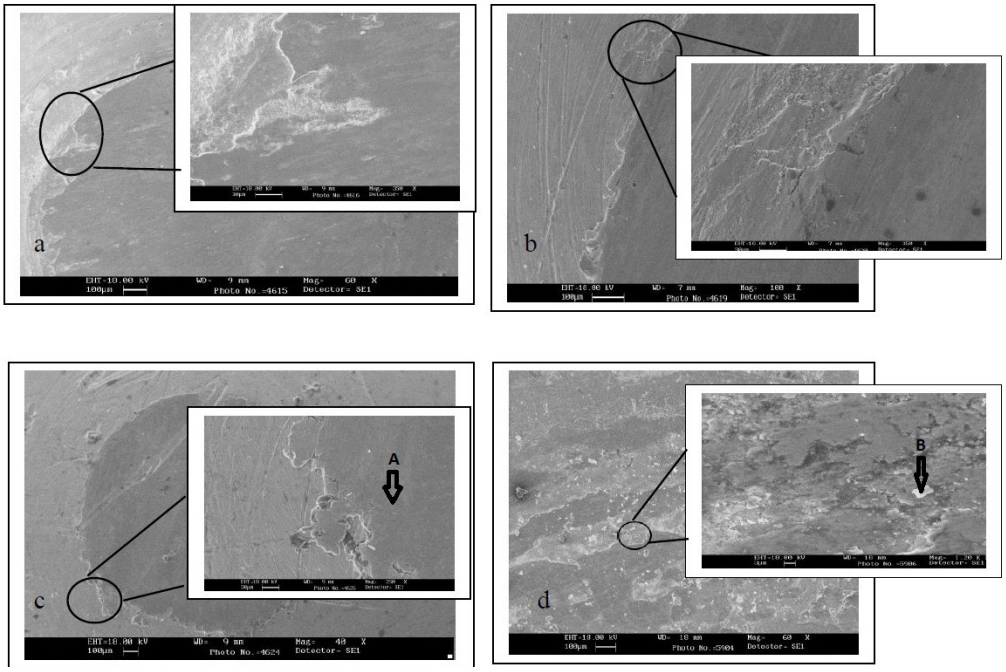

Fig. 12. Scanning electron microscopy (SEM) observations of the wear surfaces at the temperature of 550 ºC: (a) A1 (b) A2 (c) A3 and (d) H13 without coating.

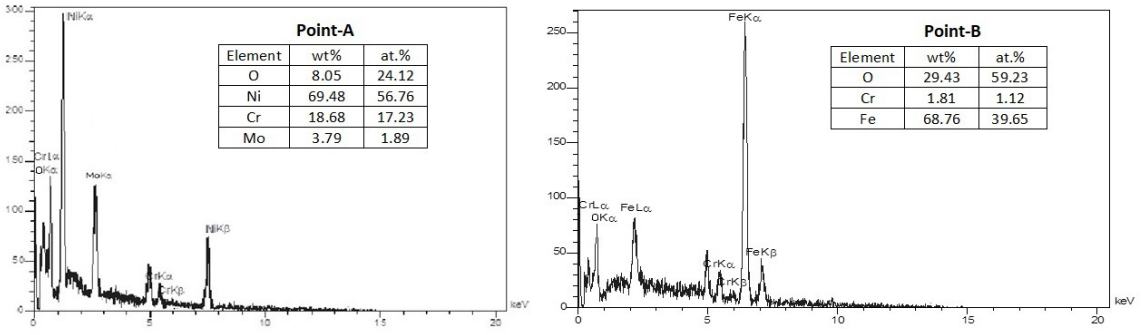

Fig. 13. EDS results of the wear surfaces at the temperature of 550 ºC, Point A in and Point B in Fig. 12-c and d.

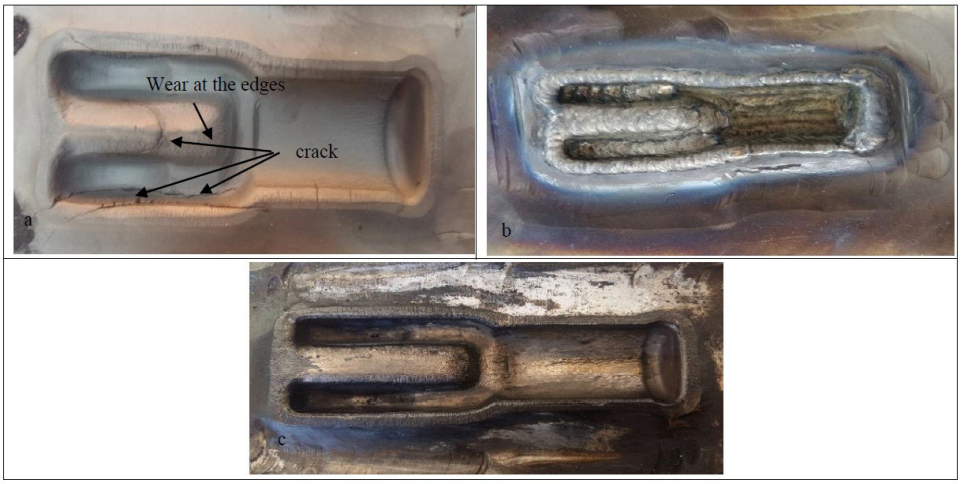

Fig.14. Procedures for performance test: (a) worn die, (b) overlaid die, (c) die after performance test.

4. Conclusion

- Inconel 625 was hardened in high temperature tests. The work hardened region supported the compacted oxide layers; therefore, it decreased the wear of the weld overlays at high temperatures about 150% compared to H13 die.
- The wear resistance of H13 alloy and the weld overlays at room temperature were increased with their room temperature hardness that it indicates an abrasive wear in this tribosystem.
- A more solid compacted layer was formed on the surface of Inconel 625 with pulsed parameters, resulting in the lowest wear among the other weld overlays at 550 ºC.
- The average die life was improved significantly with an increase of 86%, as compared to the H13 tool steel die without cladding that indicates pulsed situation can effectively use in repairing welding and cladding of the steel studied in this research.

References

[1] D. H. Ko, B. H. Kang, D. C. Ko, B. M. Kim: J. Mech. Sci. Tech., 27(2013), 153.
[2] H. Kashani, A. Amadeh, M. R. Vatanara: Mater. Sci. Technol., 24(2008), 356.
[3] L. Cser, M. Geiger, K. Lange, J. A. S. Kals: J. Eng. Manuf., 207(1993), 223.
[4] M.Terèelj, P. Panjan, P. Fajfar, R. Turk: Surf. Coat. Technol., 200(2006), 3594.
[5] M. Farhani, A. Amadeh, H. Kashani, A. Saeed-Akbari: Mater. Sci. Forum., 30(2006), 212.
[6] G. P. Dinda, A. K. Dasgupta, J. Mazumder: Mat. Sci. Eng., 509(2009), 98.
[7] K. Lange, L. Cser, M. Geiger, J. A. S. Kals: Annals of CIRP-Manuf. Technol., 41(1992), 667.
[8] P. Panjan, I. Urankar, B. Navinšek, M. Terèelj, R. Turk, M. Cekada, V. Leskovšek: Surf. Coat. Technol., 151-152(2002), 505.
[9] I. Ebrahimzadeh, F. Ashrafizadeh: Ceramics International, Vol. 40, Issue 10, Part B., (2014), 16429.
[10] I. Ebrahimzadeh, F. Ashrafizadeh, J. Mater. Eng. Perform., 24(2015), 529.
[11] I. Ebrahimzadeh, F. Ashrafizadeh, Int. J. Adv. Manuf. Tech., 77(2015), 609.
[12] D-G. Ahn: Inter. J. Precision Eng. Manuf., 14(2013), 1271.
[13]H. Kashani, A. Amadeh, H. M. Ghasemi: Wear, 262(2007), 800.
[14] K. Weman: Welding Processes Handbook, CRC Press LLC, New York, 2003.
[15] B. Cary, S. C. Helzer, Modern Welding Technology, Pearson Education, Upper Saddle River, New Jersey, 2005.
[16] A. S. C. M. D'Oliveira, R. S. C. Paredes, R. L. C. Santos: J. Mater. Process. Technol., 171(2006), 167.
[17] F. Madadi, F. Ashrafizadeh, M. Shamanian: J. Alloys Compd., 510(2012), 71.
[18] J. Cornu: Advanced Welding System, TIG and Related Processes, Vol. 3, Springer, Heidelberg, (1988), 61.
[19] A. S. C. M. D'Oliveira, R. Vilar, C. G. Feder, Appl. Surf. Sci., 201(2002), 154.
[20] J. Jiang, F .H. Stott, M. M. Stack: Wear., 256(2004), 973.
[21] Q. Ming, L. C. Lim, Z. D. Chen: Surf. Coat. Technol., 106(1998), 174.
[22] S. J. Kim, J. K. Kim: J. Nucl. Mater. 288(2001), 163.
[23] B. AlMangour, D. Grzesi, k-M. Yangb, J. Mater. Process. Technol., 244(2017), 344.